Transport of bacteria in unsaturated porous media

Anke Schäfer [a,1], Petr Ustohal [b], Hauke Harms [a,*], Fritz Stauffer [b],
Themistocles Dracos [b], Alexander J.B. Zehnder [a]

[a] *Swiss Federal Institute for Environmental Science and Technology (EAWAG) and Swiss Federal Institute of
Technology (ETH), Überlandstrasse 133, CH-8600 Dübendorf, Switzerland*
[b] *Institute of Hydromechanics and Water Resources Management, Swiss Federal Institute of Technology,
CH-8093 Zürich, Switzerland*

Abstract

Bacterial mobility in unsaturated soils plays an important role in bioremediation, biofacilitated transport of pollutants, and dispersal of pathogenic microorganisms. A sand column equipped with ports for measuring water pressure and water saturation has been used to study bacterial transport under well-defined unsaturated flow conditions. Bacterial breakthrough curves at various water saturations were obtained for two soil bacteria. Retention of hydrophobic *Rhodococcus* sp. C125 and mesohydrophilic *Pseudomonas putida* mt2 was markedly increased at lower water saturation. A mechanistic model for bacterial transport under unsaturated conditions is proposed. The model attributes stronger bacterial retention under unsaturated conditions to the accumulation of bacteria at the air–water interface. Moreover, the model takes into account changes in the available surface areas of both the solid surface and the air–water interface due to coverage by bacteria and changes in the water flow. Application of the model to our own data and data from the literature showed that short-term breakthrough experiments can be simulated, but that the model deviates from experimental observation in long-term experiments. Reasons for this deviation are discussed, and suggestions for a further model extension are made. All investigated colloidal particles had a higher affinity to the air–water interface than to the solid surface. Therefore, trapping of bacteria by air–water interfaces is an important process possibly controlling bacterial transport in unsaturated soils. © 1998 Elsevier Science B.V. All rights reserved.

Keywords: Adsorption; Bacteria; Mathematical models; Porous material; Unsaturated zone

---

* Corresponding author. Department of Microbiology, Swiss Federal Institute for Environmental Science and Technology (EAWAG), Überlandstrasse 133, CH-8600 Dübendorf, Switzerland. Tel.: +41-1-823-5519; fax: +41-1-823-5547; e-mail: hauke.harms@eawag.ch

[1] Present address: Dept. of Geography and Environmental Engineering, The Johns Hopkins University, Baltimore, MD 21218, USA.

1. Introduction

The transport of bacteria in subsurface environments has received considerable attention during the last decade. Widespread concerns include the transport of pathogenic or genetically engineered bacteria into groundwater reservoirs, and the spreading of hazardous pollutants, heavy metals and radionuclides by colloid-facilitated transport (Champ, 1986; McCarthy and Zachara, 1989). On the other hand, in situ bioremediation techniques sometimes require the introduction of specialized bacteria (Rittmann, 1994). It is crucial for the success of such activities that the introduced bacteria reach the area of contamination. Therefore, knowledge about factors affecting the movement of bacteria is required.

Bacteria are transported by the flowing water and may be retained as they interact with interfaces. Attachment of bacteria to solid surfaces has been explained by the DLVO-theory of colloidal stability (Derjaguin and Landau, 1941; Verwey and Overbeek, 1948), which describes the interaction between the negatively charged bacteria and negatively charged solid surfaces as a sum of attractive Van der Waals forces and repulsive electrostatic forces. Hydrophobic interactions (Tsao et al., 1993) between particles and cells can additionally promote attachment. Furthermore, attractive and repulsive forces have not only been considered for bacteria, but also on the level of bacterial surface polymers, which can either promote or hinder bacterial attachment (Rijnaarts et al., 1995b). The sum of these interactions can explain the retention of bacteria in water-filled porous media.

Transport of microorganisms into aquifers likely involves the passage through the vadose zone. The presence of air as an additional phase entails the presence of air–water interfaces. It has been known for a long time that bacteria tend to accumulate at the air–water interface (Blanchard and Syzdek, 1972; Marshall and Cruickshank, 1973; Dahlbäck et al., 1981; Powelson and Mills, 1996), which suggests an influence of soil air on bacterial transport. However, the number of studies reporting on such an influence is scarce. Huysman and Verstraete (1993) found an influence of the irrigation method on bacterial movement through columns filled with unsaturated soil. Wan et al. (1994) measured the breakthrough of bacteria through unsaturated sand columns and visualized the accumulation of bacteria at air bubbles. To our knowledge, so far only one paper made the attempt to model colloid transport in unsaturated porous media (Corapcioglu and Choi, 1996), although some recent conference presentations showed the growing interest in unsaturated microbial transport (Jewett et al., 1996; Wan and Tokunaga, 1996; Wilson et al., 1996).

Factors influencing bacterial movement can be identified by the application of mechanistic transport models, such as the advection–dispersion equation extended by a sink term accounting for attachment (Gerba et al., 1991; Lindqvist and Bengtsson, 1991). Whereas the clean-bed colloid filtration theory implies a constant bacterial deposition rate throughout the experiment (Harvey and Garabedian, 1991; Martin et al., 1992), other models try to account for a reduction in deposition rate as a function of bacterial surface coverage (Liu et al., 1995; Rijnaarts et al., 1996). Here, we report on a further development of the latter approach applied to unsaturated conditions.

One of the main problems in investigating unsaturated bacterial transport is the set-up and maintenance of column systems with unsaturated steady-state flow and uniform water saturation. An important objective of this work was the establishment of an experimental setup combining controlled hydraulic proceedings with the convenient monitoring of bacterial breakthrough and hydraulic conditions throughout the experiment. Collaboration between microbiologists and hydrodynamicists in the framework of the OPUS-project allowed us to measure breakthrough curves of two bacterial strains with different surface properties in quartz sand columns under various water saturations. Experiments were run under well-defined and continuously controlled hydraulic conditions. To interpret the data, we have developed a mechanistic model that accounts for the accumulation of bacteria at solid surfaces and air–water interfaces during their transport through an unsaturated porous medium and for a gradual surface coverage of both surfaces. Additionally, we have used experimental data from the literature to further evaluate the applicability of our model.

2. Materials and methods

2.1. Chemicals and buffers

All chemicals were purchased from Fluka Chemie (Buchs, Switzerland). Phosphate buffered saline (PBS) solution of pH 7.2 and of an ionic strength of 10 mM consisted of 0.493 g l^{-1} NaCl, 0.029 g l^{-1} KH_2PO_4, and 0.118 g l^{-1} K_2HPO_4. Media and PBS buffer were prepared with deionized water (NANO-pure cartridge system, Skan, Basel, Switzerland).

2.2. Bacterial strains

Two bacterial strains were used in this study: *Rhodococcus* sp. C125 (former *Corynebacterium* sp. C125) had been isolated by Schraa et al. (1987) from river Rhine sediment. *Pseudomonas putida* mt2 was first described by Williams and Worsey (1976). Both strains were cultivated on nutrient broth (Labo-Life, Pully, Switzerland) (8 g l^{-1}) in Erlenmeyer flasks on a rotary shaker at 180 rpm and 30°C. Bacteria were harvested in the early stationary phase by centrifugation for 10 min at $8500 \times g$ and 4°C. After washing the cells twice with 10 mM PBS, they were resuspended in a small volume of PBS and stored on ice until the experiments were started (within 3 h).

2.3. Physicochemical characterization of bacteria

Cell surface hydrophobicity and electrophoretic mobility are the most important surface parameters influencing bacterial adhesion (van Loosdrecht et al., 1987a). The cell surface hydrophobicity was determined by measuring the surface contact angle as described by van Loosdrecht et al. (1987b). Briefly, the cells were collected by filtering them through 0.45-μm-pore-size Micropore filters (Schleicher & Schuell, Dassel, Germany). The filters were fixed on glass slides and allowed to dry for 2 h at room

temperature. Drops of water were placed on the bacterial lawns and static contact angles, θ_w, were immediately measured with a microscope equipped with a goniometric eyepiece (G1, Krüss, Hamburg, Germany). The electrophoretic mobility u of the bacterial cells was measured with a Doppler electrophoretic light scattering analyzer (Zetamaster, Malvern Instruments, Worcestershire, UK) in 10 mM PBS at pH 7.2. Values of u were converted to zeta potentials ζ by the method of Helmholtz–Smoluchowski (Hiemenz, 1986).

The cell sizes of more than 100 bacteria were measured with a phase contrast light microscope connected to a video camera. Surface tensions of PBS and of bacterial suspensions were measured with a plate device (Dynamic Contact Angle Analyzer DCA-322, Cahn Instrument, CA, USA) according to the Wilhelmy technique (Adamson, 1990).

2.4. Column: set-up and experiments

We used a cylindrical PVC column (length: 20 cm; internal diameter: 5.34 cm) for the bacterial transport experiments. The column was equipped with a sprinkling device to homogeneously supply buffer or bacterial suspensions at the upper boundary (Fig. 1), which ensured a controlled and regular flow rate under both saturated and unsaturated conditions. The lower boundary consisted of a polyester membrane (pore size: 15 μm) that was permeable for the bacteria and allowed suctions up to 7 kPa. The column had two ports at 3.7 cm and 13.7 cm from the lower boundary for measuring water pressure by tensiometers (Ustohal et al., 1998). At the same two levels, the water saturation (S_w)
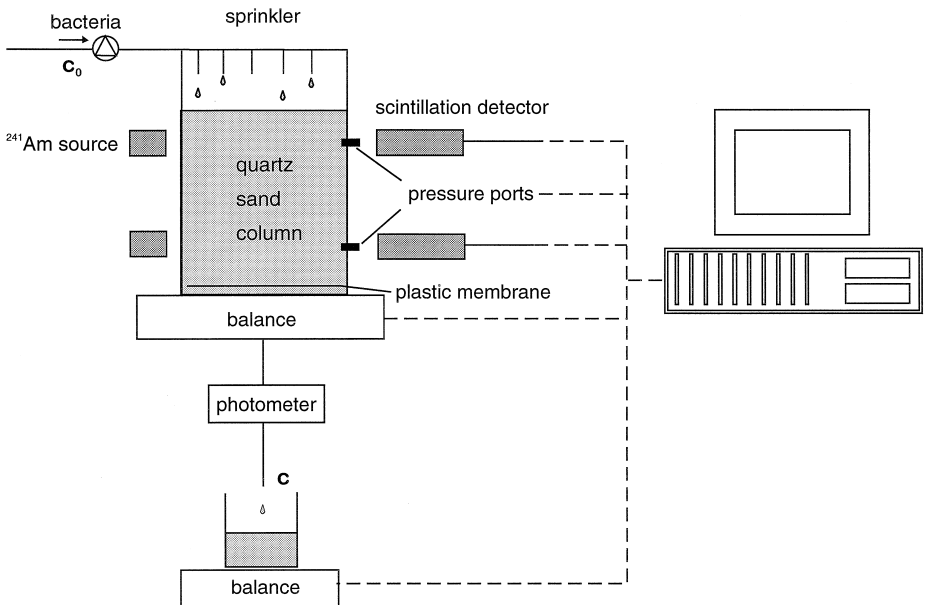

Fig. 1. Set-up of column experiments

could be measured by the γ-ray attenuation technique using ^{241}Am-sources as described by Stauffer and Dracos (1986). The water weight of the column and the flow rate were continuously measured by balances.

The column was freshly packed for each experiment using quartz sand of grain sizes between 250 and 500 μm (Zimmerli Mineralwerk, Zürich, Switzerland). The packing had a length of 15.8 cm. To achieve a high packing density, the column was dry-packed with a special packing device described by Stauffer and Dracos (1986). The column was completely saturated by air evacuation and subsequent flushing with degassed tap water. For the experiments under unsaturated conditions, the column was later drained and imbibed again overnight to $S_w = 0.86$ (that means 86% of the pore volume filled with water). This is the natural maximum water saturation for infiltration in unsaturated sand, because residual air bubbles remain trapped in the matrix. To achieve a lower S_w, the column was further drained by reducing the inflow rate and applying suction by gradually lowering the outflow level, according to the steady state head control method (Klute and Dirksen, 1986). When unsaturated steady-state flow with S_w, as uniform as possible (deviation of S_w at upper and lower port from overall S_w maximally 9%), was achieved, the column was equilibrated with at least 6 pore volumes PBS. Table 1 shows the parameters of the column experiments. In a second set of experiments, breakthrough curves of 100 ppm $CaCl_2$ as a conservative tracer were monitored with a modified electrical conductivity meter at various water saturations (Metrohm, Herisau, Switzerland) (Ustohal et al., 1998). They were used to determine the dispersion coefficients D at the different water saturations by parameter fitting. The porosity ϕ was determined gravimetrically.

For the experiments at $S_w = 1$ and 0.86, which represent the natural maximum water saturations for infiltration into fully saturated and unsaturated sand, respectively, an inflow rate Q of 12.2 ml min^{-1} was chosen (both saturations can be maintained at an optional flow rate). On the other hand, under less saturated conditions Q was controlled by the applied drainage regime, which is the combination of inflow reduction and suction increase. Water pressure and saturation S_w at the upper and lower ports, total water weight, and Q were recorded throughout the experiments. The water weight was used to calculate the average S_w gravimetrically. Table 2 shows mean values of S_w and the flow velocities v (cm min^{-1}). Concentrated bacterial suspensions were diluted with 10 mM PBS to give inflow concentrations c_0 of an absorbance at 280 nm, A_{280}, of

Table 1
Parameters of the column experiments

Parameter	Value
Sand grain size	250–500 μm
Calculated surface area of sand	60.6 cm^2 g^{-1}
Bulk density	1.61 g cm^{-3}
Porosity	0.39
Total column pore volume	136.7 ml
Ionic strength	10 mM
pH	7.2

Table 2
Parameters of the individual experiments

Bacterial strain	Experiment	S_w^a	S_w at upper port[b]	S_w at lower port[b]	Q [cm^3 min^{-1}]	v [cm min^{-1}]	D [cm^2 min^{-1}]
Rhodococcus sp. C125	1	1			12.2	1.41	0.026
	2	0.86	0.86	0.86	12.2	1.64	0.031
	3	0.69	0.64	0.77	8.4	1.41	0.149
P. putida mt2	4	1			12.2	1.41	0.026
	5	0.86	0.86	0.86	12.2	1.64	0.031
	6	0.63	0.60	0.68	10.8	1.98	0.210

[a] Determined gravimetrically by measuring the water weight.
[b] Determined by γ-ray attenuation.

0.58 ± 0.02, corresponding to about 4.4×10^7 cells ml^{-1} of *Rhodococcus* sp. C125 and 8.7×10^7 cells ml^{-1} of *P. putida* mt2. A step input of 8.3 ± 0.2 water pore volumes $\phi V_c S_w$ of bacterial suspension was applied to the column with V_c as the total column volume (cm^3). Bacterial concentration in the effluent was determined by measuring A_{280} every minute with a spectrophotometer (CADAS, Dr. Lange, Berlin, Germany) equipped with a flow-through cuvette. c_0 remained constant throughout the experiments. After flushing the column with 4 pore volumes of PBS, the effluent was free of bacteria, and the experiments were stopped. Experiments under saturated conditions ($S_w = 1$) were repeated and shown to be reproducible. Breakthrough curves were corrected for a baseline drift downwards that occurred when the bacteria were applied to the column. Photometric and microscopic experiments showed that the UV-absorption background caused by colloids that detached from the sand was reduced to about 40% within one pore volume when a bacterial pulse was applied (data not shown). The bacteria stabilized the colloids on the sand.

2.5. Modeling approach

Bacterial breakthrough curves were analyzed with a mechanistic transport model. Bacteria are transported with the water flow in porous media. They collide with solid particles due to convective diffusion, interception and sedimentation, and can be subject to attachment (Rijnaarts et al., 1995a). Assuming reversible attachment, bacterial transport in water-saturated columns can be described by the advection–dispersion equation extended by two terms accounting for cell sorption and desorption, respectively (Harvey and Garabedian, 1991).

$$\frac{\partial C_1}{\partial t} = D \frac{\partial^2 C_1}{\partial z^2} - v \frac{\partial C_1}{\partial z} - k_1 C_1 + k_{des} \frac{A_s \rho}{\phi} C_s \tag{1}$$

where C_1 (cells cm^{-3}) is the bacterial concentration in the liquid phase, D the apparent dispersion coefficient (cm^2 min^{-1}), k_1 (min^{-1}) the filtration constant accounting for sorption to the solid surface, k_{des} the bacterial desorption constant (min^{-1}), A_s the specific surface area of the solid phase available for adhesion (cm^2 g^{-1}), ρ the bulk

density (g cm^{-3}), C_s the bacterial concentration on the solid surface (cells cm^{-2}), z the axial coordinate (cm), and t is time (min). The accumulation of bacteria on the solid surface is a function of their depletion from the liquid phase by filtration and their possible subsequent detachment and can be described as:

$$\frac{\partial C_s}{\partial t} = k_1 \frac{\phi}{A_s \rho} C_1 - k_{des} C_s \tag{2}$$

Eq. (1) can also be used to describe unsaturated steady-state flow when changes in the volumetric water content of the matrix are taken into account. The air–water interface represents an additional sink for bacteria under unsaturated conditions, so a term accounting for this process was added. Because of the presence of large capillary forces (Williams and Berg, 1991), no detachment from the air–water interface was assumed. The general formulation of our model for unsaturated bacterial transport is

$$\frac{\partial C_1}{\partial t} = D \frac{\partial^2 C_1}{\partial z^2} - v \frac{\partial C_1}{\partial z} - k_1 C_1 + k_{des} \frac{A_s \rho}{\phi S_w} C_s - k_2 C_1 \tag{3}$$

with

$$\frac{\partial C_s}{\partial t} = k_1 \frac{\phi S_w}{A_s \rho} C_1 - k_{des} C_s$$

where k_2 accounts for adhesion to the air–water interface.

It is known that k_1 can change with time by the attachment of bacteria, which can render the solid surface less attractive for further attachment. The available deposition area on collector grains is reduced as attached bacteria exclude the immediate vicinity of the collector surface from subsequent deposition. This surface exclusion phenomenon is generally known as blocking (Johnson and Elimelech, 1995; Rijnaarts et al., 1996). Since the breakthrough curves we obtained under water-saturated conditions, where the cells could only attach to solid surfaces, apparently represented typical blocking curves due to their positive slope and their lack of tailing, we used the traditional blocking concept to describe bacterial interactions with the solid surface (Liu et al., 1995; Rijnaarts et al., 1996). Under unsaturated conditions, the presence of air may create inaccessible water films on the collector particles. To account for this decrease in solid surface area available for bacterial adhesion, we additionally included S_w as a proportionality factor in the following equations:

$$k_1 = k_{cs}\left(1 - \frac{C_s}{C_{max}}\right) S_w \tag{4a}$$

and

$$A_s = A_{s(S_w=1)} S_w \tag{4b}$$

C_{max} is the maximum attainable bacterial concentration on the solid surface (cells cm^{-2}), k_{cs} is the deposition constant for cells to the uncovered solid surface (min^{-1}), and $A_{s(S_w=1)}$ is the specific surface area of the solid phase available for adhesion at $S_w = 1$ (cm^2 g^{-1}). As C_s rises to C_{max}, the deposition rate will decrease to zero due to

competition between the bacteria. As a consequence, the maximum concentration of C_s will be equal to C_{max}. The rate of attachment to the solid surface is linearly proportional to the volumetric water fraction and the concentration of bacteria in the water phase.

We tested two model formulations of increasing complexity for their ability to describe bacterial interactions with the air–water interface. For both approaches, we assumed that k_2 is proportional to the area of the air–water interfaces, which is roughly proportional to the air content $(1 - S_w)$ for $S_w > 0.5$ (Gvirtzman and Roberts, 1991; Reeves and Celia, 1996). At $S_w < 0.3$–0.4, the area of air–water interfaces decreases again, so that the following equations are not valid any more.

$$k_{2a} = k_a(1 - S_w) \tag{5}$$

$$k_{2b} = k_{ca}\left(1 - \frac{C_a}{C_{max2}}\right)(1 - S_w) \tag{6}$$

k_a (min^{-1}) is the deposition constant for the cells to the air–water interface, k_{ca} the deposition constant for the cells to the uncovered air–water interface (min^{-1}), C_a the concentration of bacteria at the air–water interface (cells cm^{-2}), and C_{max2} the maximum attainable bacterial concentration at the air–water interface (cells cm^{-2}). While k_{2a} assumes the first-order deposition of bacteria to the air–water interface, k_{2b} takes into account that the air–water interface is partially covered by bacteria in the course of the experiment, so that only the area fraction $1 - C_a/C_{max2}$ is available for subsequent attachment. This latter formulation is mechanistically equivalent to the description of bacterial interactions with the solid surface in Eq. (4a). The accumulation of bacteria at the air–water interface is in both model suggestions caused by their depletion from the liquid phase and can be described as

$$\frac{\partial C_a}{\partial t} = k_2 \frac{\phi S_w}{A_a} C_1 \tag{7}$$

A_a (cm^2 cm^{-3}) is the specific area of air–water interfaces per column volume. Because the calculation of A_a at different water saturations is still not well-established, the following empirical relationship was developed on the basis of recent publications (Gvirtzman and Roberts, 1991; Reeves and Celia, 1996; Saripalli et al., 1997):

$$A_a = 80 \text{ cm}^2 \text{ cm}^{-3} (1 - S_w) \frac{0.025 \text{ cm}}{r} \qquad \text{for } S_w > 0.5 \tag{8}$$

r is the collector radius (cm).

The coefficients k_{2a} and k_{2b} were tested with the breakthrough curves obtained for *Rhodococcus* sp. C125 at different water saturations. Because the measured breakthrough curves exhibited no tailing, the desorption term was omitted from Eq. (3). All fits were done with the AQUASIM computer software (Reichert, 1994) for the simulation and data analysis of aquatic systems. Dispersion coefficients for chloride breakthrough curves at different S_w were fitted with the advection–dispersion equation. To account for differences in flow velocity between the tracer experiments and the experiments with bacteria, the relationship $D = dv$, where d is the dispersivity, was used to calculate D for the bacterial transport experiments.

Table 3
Physicochemical properties of the colloids

Colloid	Size [μm]	Contact angle θ_w [deg]	Zeta potential ζ [mV]
Rhodococcus sp. C125	3.0×0.9	95.1±1.7	−44.8±1.4
P. putida mt2	2.2×0.9	38.2±1.5	−13.4±1.0
P. cepacia 3N3A[a]	1.3×0.8	24.7±3.1	−12.1
Arthrobacter sp. S-139[a]	1.0×0.8	77.1±2.5	−56.3
Latex particles[b]	0.22	127±5	−36

[a] From Wan et al. (1994).
[b] From Wan and Wilson (1994).

2.6. Analysis of literature data

The model was tested on a set of data from the literature on transport of *Pseudomonas cepacia* 3N3A, *Arthrobacter* sp. S-139 (Wan et al., 1994) and hydrophobic latex particles (Wan and Wilson, 1994) in unsaturated sand columns. Physicochemical parameters of the colloids and parameters of the column experiments are listed in Tables 3 and 4. Because only the bacterial breakthrough curves of the latex particles showed considerable tailing, the desorption term of Eq. (3) was omitted for the other two cases. The experiments had been conducted at $S_w = 1$ (a), 0.86 (b), 0.54 (c), and $v = 10$ cm h^{-1}. Dispersion coefficients were deduced from the breakthrough data as 0.0026 (a), 0.0028 (b), 0.1 (c) cm^2 min^{-1}.

2.7. Sensitivity analysis

A sensitivity analysis of our model formulated with k_{2b} was carried out to determine the relative contributions of each of the fitting parameters, k_{cs}, C_{max}, k_{ca}, and C_{max2} on the model output. Proceeding from the fitted breakthrough curve of *Rhodococcus* sp. C125 at $S_w = 0.86$, each parameter was varied individually while the other three were kept constant.

Table 4
Parameters for the column experiments from Wan and Wilson (1994) and Wan et al. (1994)

Parameter	Experiments with bacteria	Experiments with latex particles
Sand grain size	212–315 μm	212–315 μm
Calculated surface area of sand	86.3 cm^2 g^{-1}	86.3 cm^2 g^{-1}
Bulk density	1.56 g cm^{-3}	1.65 g cm^{-3}
Porosity	0.41	0.43
Column diameter	2.5 cm	2.5 cm
Column length	30 cm	30 cm
v	10 cm h^{-1}	10 cm h^{-1}

3. Results

3.1. Physicochemical properties

Physicochemical properties of all colloids are listed in Table 3. *Rhodococcus* sp. C125 and the latex particles are very hydrophobic, *Arthrobacter* sp. S-139 moderately hydrophobic, *P. putida* mt2 mesohydrophilic and *P. cepacia* 3N3A hydrophilic. The two hydrophilic bacteria are less negatively charged than the two hydrophobic bacteria. The latex particles as most hydrophobic colloids are only intermediately negatively charged.

Surface tensions (advancing) were 72.2×10^{-5} N cm^{-1} for deionized water, $(72.1 \pm 0.2) \times 10^{-5}$ N cm^{-1} for PBS, $(72.2 \pm 0.1) \times 10^{-5}$ N cm^{-1} for a suspension of *Rhodococcus* sp. C125 and $(72.1 \pm 0.8) \times 10^{-5}$ N cm^{-1} for a suspension of *P. putida* mt2.

3.2. Breakthrough curves of Rhodococcus sp. C125 and P. putida mt2

Pulses of 8.3 ± 0.2 pore volumes of bacterial suspension were applied to the column at different S_w. The parameters of the column experiments in general and of the individual experiments are listed in Tables 1 and 2. Independent experiments in saturated systems showed that the differences between flow velocities in the individual experiments (Table 2) had no influence on the adhesion of *Rhodococcus* sp. C125 (data not shown). However, for *P. putida* mt2 slightly less bacteria adhered at higher flow velocities.

Breakthrough curves of *Rhodococcus* sp. C125 at different S_w are shown in Fig. 2a and b. The curve measured under full saturation has a linear positive slope indicating that the solid surface was rendered less attractive by attached bacteria. A comparison with the breakthrough curves monitored at $S_w = 0.86$ and $S_w = 0.69$ reveals that dramatically less bacteria were transported through the columns at lower S_w. More bacteria were retained on the column at $S_w = 0.69$ than at $S_w = 0.86$. Mass recoveries in the effluent for *Rhodococcus* sp. C125 were 31.9% under fully saturated conditions, 9.7% at $S_w = 0.86$ and 3.2% at $S_w = 0.69$. It seems that under unsaturated conditions bacteria accumulate at the air–water interfaces. Entrapped air volumes and, thus, also air–water interfaces are believed to be static and non-connecting for $S_w > 0.6$ (Dury et al., 1998).

The deposition behavior of *P. putida* mt2 under saturated conditions indicates a strong nonlinear decrease in solid surface attractiveness (Fig. 3). Many more cells were transported under saturated than under unsaturated conditions, but virtually no difference could be seen between the breakthrough curves obtained at $S_w = 0.86$ and $S_w = 0.63$. Mass recoveries in the effluent were 15.5% under saturated conditions, 5.8% at $S_w = 0.86$ and 6.4% at $S_w = 0.63$. We think that also for *P. putida* mt2 the additional amount of bacteria that is retained under unsaturated conditions is due to the bacterial accumulation at the air–water interface. One contribution to the lack of difference
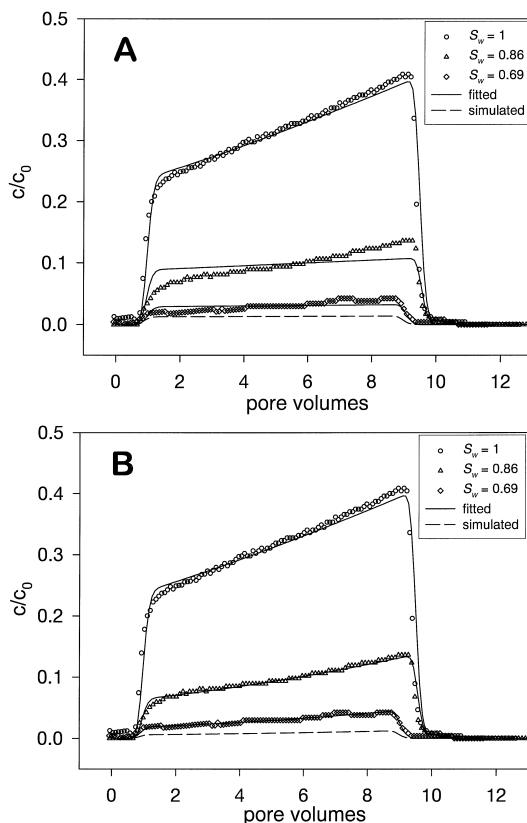
Fig. 2. Observed breakthrough curves for *Rhodococcus* sp. C125. Modeling results were obtained with Eq. (3) using bacterial deposition rates k_{2a} (A) or k_{2b} (B). Parameters for bacterial sorption to the solid–water interface were fitted by using their breakthrough at $S_w = 1$ and used for all other curves. Parameters for their attachment to air–water interfaces were fitted by using the breakthrough at $S_w = 0.86$ or 0.69. Additionally, fitted values for interaction with air–water interfaces at $S_w = 0.86$ were used to simulate breakthrough for $S_w = 0.69$.

between transport for this strain at $S_w = 0.86$ and $S_w = 0.63$ could be that slightly less bacteria can adhere due to the higher flow velocity at lower S_w.

3.3. Hydraulic data

The hydraulic data of the unsaturated experiments with a mean water saturation of $S_w = 0.69$ and $S_w = 0.63$ show an increase in saturation with time. The breakthrough experiment with *Rhodococcus* sp. C125, which can be seen exemplarily in Fig. 4, exhibited an increase from $S_w = 0.663 \pm 0.002$ to $S_w = 0.710 \pm 0.004$. In the experiment with *P. putida* mt2, S_w increased from $S_w = 0.610 \pm 0.002$ to $S_w = 0.649 \pm 0.003$. In both experiments the water saturation remained constant when pure buffer instead of cells was applied to the column. The increase in water saturation was in correspondence with a decrease in hydraulic pressure as measured with the tensiometers.
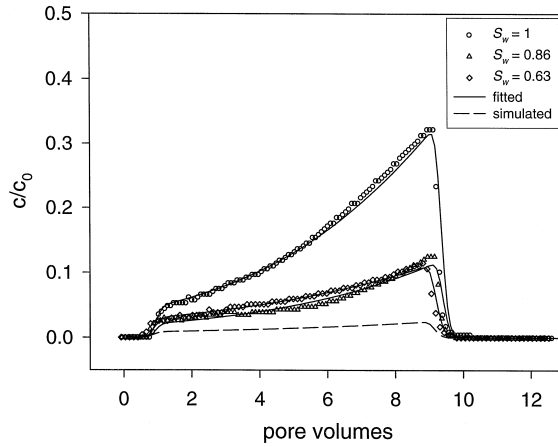
Fig. 3. Observed breakthrough curves for *P. putida* mt2 and modeling results obtained with Eq. (3) using k_{2b}. Parameters were fitted as described in the legend of Fig. 2.

Gravimetric and γ-ray attenuation measurements of S_w were approximately in agreement. However, the saturation measurements at the top and the bottom of the column by γ-ray attenuation cannot be omitted in unsaturated column experiments. They are crucial for the control of the degree of uniformity of the saturation over the whole column. The mean value between the water saturations measured by γ-ray attenuation at the column top and bottom is similar to the mean column water saturation determined gravimetrically, but shows, as expected, larger scatter. Fig. 4 shows that the gravimetric water saturation is always slightly lower than the mean value between the saturations at the upper and lower measuring port. This indicates a nonlinear water saturation profile. Probably some water is dammed right above the lower boundary. Additionally, one can observe that the higher S_w at the bottom of the column is always accompanied by a higher hydraulic pressure as compared to the top. The fact that obviously more pressure is necessary to drain the bottom of the column than the top indicates a slightly nonuniform column packing.
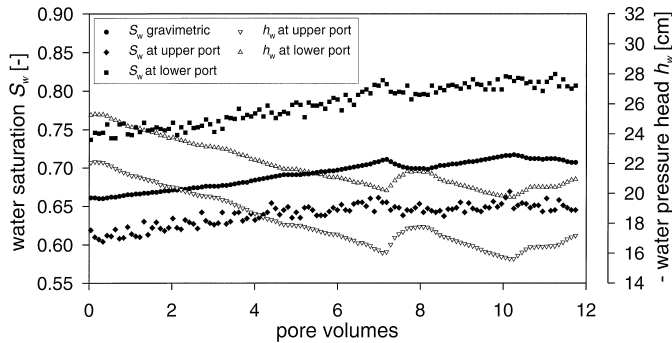

Fig. 4. Hydraulic data for the column experiment with *Rhodococcus* sp. C125 at $S_w = 0.69$

3.4. Modeling of breakthrough curves

Fig. 2a shows the application of Eq. (3) with k_{2a} to the breakthrough curves of *Rhodococcus* sp. C125. Parameters for the adhesion of bacteria to the solid surface (k_{cs}, C_{max}) were fitted with the breakthrough curve obtained for fully saturated conditions and then applied to both unsaturated breakthrough curves. The deposition rate for bacteria to the air–water interface (k_a) was fitted with the breakthrough data at $S_w = 0.86$. It is obvious that it is not possible to describe the slope of this breakthrough curve satisfyingly with Eq. (3) using a constant deposition rate for the air–water interface. The breakthrough curve at $S_w = 0.69$ was either modeled by fitting k_a or simulated using the same k_a as for the breakthrough curve at $S_w = 0.86$. Fig. 2a shows that the transport of bacteria at lower S_w is considerably underestimated by the model when the same set of parameters is used for all three curves. When k_a is adjusted again with the breakthrough curve at $S_w = 0.69$, the amount of transported bacteria can be described properly, but the slope of the curve does not suit the data. All fitted parameters are listed in Table 5.

Fig. 2b shows that Eq. (3) using k_{2b} is much better suited for the description of bacterial transport under unsaturated conditions: with this more complex model the slope of the *Rhodococcus* sp. C125 breakthrough curves at $S_w = 0.86$ and at $S_w = 0.69$ could be described. However, the model with k_{2b} also underestimated bacterial transport at $S_w = 0.69$ when the same set of parameters was used as at $S_w = 0.86$. All further fits with Eq. (3) were conducted using k_{2b}. Fitted parameters are listed in Table 5.

Fig. 3 shows the application of our model to the breakthrough curves of *P. putida* mt2. Although the saturated breakthrough curve has a nonlinear slope, it could be described well by the model. The model also allowed an acceptable fit for the breakthrough curves of *P. putida* mt2 at $S_w = 0.86$ and $S_w = 0.63$. When breakthrough of *P. putida* mt2 at $S_w = 0.63$ was simulated with the parameters fitted at $S_w = 0.86$, bacterial transport was underestimated. The higher flow velocity in this experiment might slightly reduce bacterial adhesion due to their shorter residence time in the

Table 5
Estimates of model parameters

Colloid	Parameter was fitted at S_w	k_{cs} [min^{-1}]	C_{max} [cells cm^{-2}]	k_a [min^{-1}]	k_{ca} [min^{-1}]	C_{max2} [cells cm^{-2}]	k_{des} [min^{-1}]
Rhodococcus sp. C125	1	0.127	2.7×10^6				–
	0.86			1.030	1.273	1.4×10^7	
	0.69			0.767	0.906	7.5×10^6	
P. putida mt2	1	0.275	3.6×10^6				–
	0.86				1.230	1.3×10^7	
	0.63				0.756	5.4×10^6	
Arthrobacter sp. S-139	1	0.002	2.0×10^8				–
	0.85				0.020	2.9×10^7	
P. cepacia 3N3A	1	0.0004	1.5×10^9				–
	0.85				0.003	2.5×10^6	
Latex particles	1	0.003	1.3×10^{10}				0.0002
	0.85				0.148	1.7×10^6	
	0.54				0.055	6.7×10^5	

column, but is insufficient to explain the full extent of deviation between model and breakthrough data. Fitted parameters are listed in Table 5.

A comparison of the fitted parameters for the two strains shows that hydrophilic *P. putida* mt2 has a higher affinity to the sand surface than hydrophobic *Rhodococcus* sp. C125. The affinities to the air–water interface are similar for both strains and are five- to ten-fold higher than their affinities to the solid surface. C_{max} is similar for both bacteria and is already reached when about 6% of the total surface are covered by bacteria, signaling significant blocking of the area around the attached cells. C_{max2} is considerably higher than C_{max}, which leads to the conclusion that blocking phenomena are of minor importance on the air–water interface. This seems to make sense since, in contrast to cells attached to the solid surface, cells in the air–water interface are laterally still mobile and tend to form aggregates (Williams and Berg, 1991). However, all absolute C_{max2} values have to be regarded with caution because still no consensus about the absolute area of air–water interface in unsaturated column systems is reached, as the diverging literature values reveal (Gvirtzman and Roberts, 1991; Reeves and Celia, 1996; Saripalli et al., 1997).

3.5. Modeling of literature data

To further test the applicability of our model, we applied it to data from the literature. Wan et al. (1994) described the transport of pulse inputs of hydrophilic and hydrophobic bacteria in saturated and unsaturated sand-filled columns. Our fitting and simulation, respectively, of the breakthrough curves are shown in Fig. 5 for hydrophilic *P. cepacia* 3N3A and in Fig. 6 for hydrophobic *Arthrobacter* sp. S-139. The breakthrough curves at $S_w = 1$ and $S_w = 0.86$ could be fitted well, and the breakthrough curves at $S_w = 0.54$ could be simulated successfully by using these fitted parameters.

The application of our model to long-term breakthrough experiments with hydrophobic latex particles (Wan and Wilson, 1994) (Fig. 7) shows that breakthrough at $S_w = 1$,
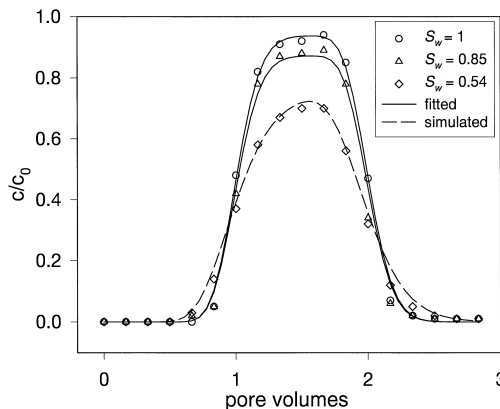

Fig. 5. Breakthrough of one pore volume of hydrophilic *P. cepacia* 3N3A through sand columns as reported by Wan et al. (1994). Parameters were fitted as described in the legend of Fig. 2.
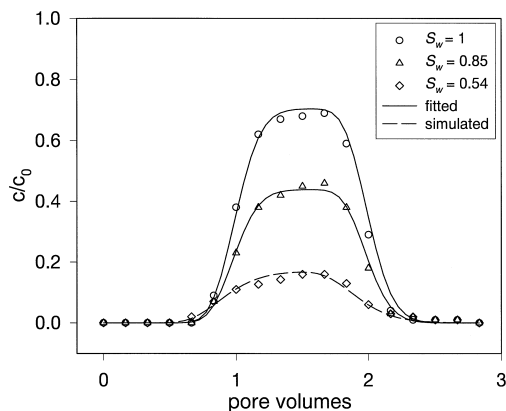
Fig. 6. Breakthrough of one pore volume of hydrophobic *Arthrobacter* sp. S-139 through sand columns as reported by Wan et al. (1994). Parameters were fitted as described in the legend of Fig. 2.

$S_w = 0.86$ and $S_w = 0.54$ could be fitted well except for the tailing, whereas simulation of breakthrough at lower saturation using the fitted parameters clearly underestimated the observed outflow concentration. The fitting of the tailing probably could be improved when nonlinear desorption processes would be included. All fitted parameters are listed in Table 5.

It is striking that k_{cs} obtained for both bacteria and the latex particles are much smaller than those found in our experiments. A possible reason for this may be that rigorous washing of the sand used by Wan and coworkers (Wan and Wilson, 1994; Wan et al., 1994) diminished bacterial and colloidal attraction to its surface. On the other hand, both bacterial strains used by Wan and coworkers, and especially the latex particles, are much smaller than the strains used by us, leading to less straining of the colloids in the column. This fact could also account for the phenomenon that likewise
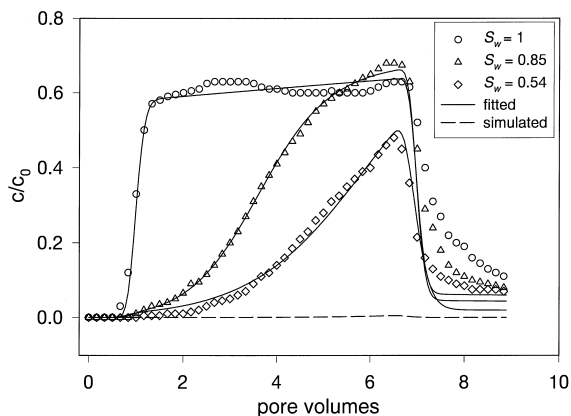

Fig. 7. Breakthrough of six pore volumes of hydrophobic latex particles through sand columns as reported by Wan and Wilson (1994). Parameters were fitted as described in the legend of Fig. 2.

k_{ca} is much smaller for the experimental system used by Wan and coworkers than for our system. It is noticeable, however, that for all types of colloids investigated, k_{ca} is larger than k_{cs}, meaning that the affinity to the air–water interface is always larger than the affinity to the solid surface. Additionally, it can be seen that k_{cs} as well as k_{ca} increase with increasing colloid hydrophobicity. The fitted values of C_{max} and C_{max2} for *Arthrobacter* sp. S-139 and *P. cepacia* 3N3A are not very meaningful because of the short duration of these experiments that makes it difficult to estimate them correctly. The values for the latex particles are remarkable in so far as C_{max} is 4 orders of magnitude larger than C_{max2}. The high C_{max} value can at least partially be explained by the extremely small particle size. The small C_{max2} could be a hint for the contribution of a size dependent mechanism to the retention of colloids under unsaturated conditions, for example straining by thin water films.

3.6. Sensitivity analysis

The results of the fitted breakthrough curve of *Rhodococcus* sp. C125 at $S_w = 0.86$ (Fig. 2b) were taken as reference to examine the effects on the predicted breakthrough
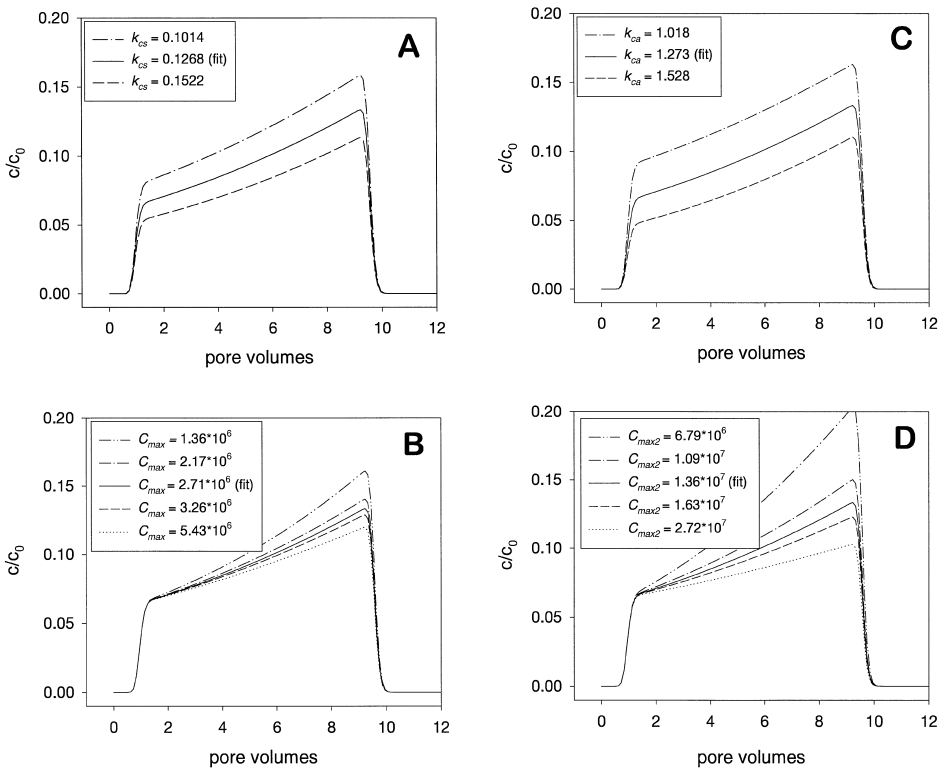

Fig. 8. Calculated breakthrough curves for *Rhodococcus* sp. C125 at $S_w = 0.86$. In each plot, either k_{cs} (A), C_{max} (B), k_{ca} (C), or C_{max2} (D) was varied while all other parameters were kept unchanged.

curves of increasing and decreasing the four fitting parameters k_{cs}, C_{max}, k_{ca}, and C_{max2} by 20 to 100% (Fig. 8). An increase or decrease of k_{cs} by 20% effectively influences the predicted breakthrough curve by changing the initial breakthrough concentration while leaving the slope of the curve constant (Fig. 8a). C_{max} has to be halved or doubled before a distinct change in the predicted curve can be observed (Fig. 8b). Changes in C_{max} leave the initial breakthrough concentration constant, but influence the slope of the curve. It is obvious from Fig. 8a and b that changes in k_{cs} and C_{max} influence the shape of the breakthrough curve in independent ways, so that the two parameters do not correlate. Because the equations for bacterial interactions with the solid surface and the air–water interface are mathematically equivalent (see Eqs. (4a) and (6)), it is not surprising that changes in k_{ca} and C_{max2} have the same effects as changes in k_{cs} and C_{max}, respectively (Fig. 8c and d). However, because k_{cs} and C_{max} can be fitted independently from k_{ca} and C_{max2} using breakthrough curves measured at $S_w = 1$, the correlations between effects of changing the two sets of parameters are not a problem. Also for bacterial interactions with the air–water interface, changes in the deposition rate k_{ca} are more effective than changes in the maximum attainable surface concentration C_{max2}.

4. Discussion

The transport of two bacterial strains, the hydrophobic *Rhodococcus* sp. C125 and the mesohydrophilic *P. putida* mt2, through porous media was strongly reduced by decreasing the water saturation. We assumed that the increased retention of both bacteria in porous media under unsaturated conditions was due to their accumulation at air–water interfaces. Wan et al. (1994) also observed a decrease of bacterial transport through unsaturated sand columns when they applied short bacterial pulses. However, because of the small quantity of bacteria applied, they were not able to examine the effect of chances of the solid surfaces and the air–water interfaces due to their partial coverage. It has been known for a while that bacteria tend to accumulate at air–water interfaces (Marshall and Cruickshank, 1973; Dahlbäck et al., 1981). The two bacteria used in this study were both shown in independent measurements to accumulate at air–water interfaces to a considerable extent (Schäfer et al., 1998). It has been proposed that long range hydrophobic interactions are responsible for the attraction between air–water interfaces and both, hydrophilic and hydrophobic colloids (Ducker et al., 1994). The lack of a difference in the transport behavior of *P. putida* mt2 between $S_w = 0.86$ and $S_w = 0.63$ could have been partly caused by the higher flow velocities at lower water saturation that reduced the bacterial residence time in the column considerably.

We have proposed a mechanistic model that describes bacterial transport in unsaturated porous media. It takes into account changes in the available surface area of both the solid surfaces and the air–water interfaces due to coverage by bacteria and changes in the water flow. Application of our model to our own breakthrough data and long-term breakthrough data from the literature (Wan and Wilson, 1994) showed that the model is appropriate to fit the data, but that the same set of parameters cannot properly describe colloidal transport at different water saturations. Under unsaturated conditions, bacterial

retention is lower at lower S_w than expected from experiments at higher S_w due to our model. However, the model was able to predict short-term breakthrough data from the literature (Wan et al., 1994). It looks like the model is still insufficient to describe long-term system changes during the experiment. We think that the parts of the model accounting for bacterial interaction with the interfaces are correct, and that discrepancies arise from the transport of bacteria in the system. One possible explanation for a reduced bacterial transport to the interfaces at lower S_w is that more immobile water portions or thin water films are formed that cannot be accessed by the bacteria. Although we tried to account for immobile water on the level of bacterial attachment to the solid surfaces, the accurate calculation of stagnant water layers as introduced by van Genuchten and Wierenga (1976) might allow for a more exact transport model. At lower water saturation, the fraction of immobile water is greater and therefore the transport of the water/the bacteria to the interfaces is reduced. However, because more parameters are introduced, more breakthrough data under unsaturated conditions would be needed to verify such an extended model. Another theory accounting for the relative increase in bacterial mobility at lower S_w might be that some air–water interfaces already start to be connecting and mobile at water saturations around 70%, therefore leading to additional transport of the bacteria in the air–water interfaces through the column.

A similar model as ours for the transport of colloids in unsaturated porous media has recently been proposed by Corapcioglu and Choi (1996), who included first-order kinetics to account for the interactions between colloids and solid surfaces and second-order kinetics for the interactions with the air–water interface. Because of the first-order approach to the interactions with the solid surface, the model is not able to describe bacterial blocking phenomena found in our case as a result of the partial coverage of the solid surfaces by bacteria. Corapcioglu and Choi also used the data from Wan et al. (1994) and Wan and Wilson (1994) to validate their model. They as well needed to adjust at least one parameter for each data set to get a satisfactory fit. However, Corapcioglu and Choi did not include mechanistic considerations about the changing areas of solid surfaces and air–water interfaces due to coverage by bacteria and changes in the water flow. Moreover, they did neither try to quantify the area of air–water interfaces, nor consider the hydraulics of the systems (e.g., D or the water saturation profile).

A comparison of the affinities of the different colloids to the solid and the air–water interfaces shows that they are only partially related to the colloidal surface properties (Tables 3 and 5). Although for all investigated colloids k_{ca} is larger than k_{cs}, only those investigated by Wan and coworkers show for both parameters an increase with increasing surface hydrophobicity (Wan and Wilson, 1994; Wan et al., 1994). Mesohydrophilic *P. putida* mt2 has a larger k_{cs} than hydrophobic *Rhodococcus* sp. C125, and the k_{ca} of both strains are similar. However, it has been shown that *Rhodococcus* sp. C125 possesses amphiphilic surface polymers that sterically hinder its attachment to silica surfaces (Rijnaarts et al., 1995b). Moreover, because of the different experimental systems and collector surfaces, it is not possible to directly compare the parameters from Wan's experiments with ours.

We have succeeded to set up a column system that is suitable for obtaining bacterial breakthrough curves under unsaturated conditions at largely controlled hydraulic condi-

tions. To our knowledge, this is the first study in which measurement of bacterial transport in unsaturated columns was accompanied by monitoring the hydraulic parameters. Exact description of the hydraulic data has shown that the water saturation of the column increased during the unsaturated experiments. The increase is not caused by a change in surface tension of the liquid in the presence of bacteria. Our hypothesis is that the bacteria lower the oxygen saturation in the buffer suspension before it is sprinkled to the column. When the oxygen-deprived bacterial suspension enters the column, it dissolves oxygen from the air in the column, thereby increasing the water saturation.

Transport of hydrophobic and hydrophilic bacteria is drastically reduced under unsaturated conditions. This fact has to be considered when specialized bacteria are introduced to soil in the course of a bioremediation process and have to pass unsaturated soil layers on their way to the target pollutants. Additionally, it should be considered that heavy rainfall can mobilize bacteria by reducing the area of air–water interfaces. Bacterial mobility could also be affected in anaerobic deeper soil layers with a high biogenic gas production. The interactions of bacteria with air–water interfaces can be expected to play a major role for microbial mobility in the capillary fringe, where air–water interfaces move with the oscillating water table. The field conditions, however, probably differ from our experimental conditions. One the one hand, bacterial numbers are usually lower in nature, rendering the surface coverage by bacteria less important. On the other hand, bacteria found in the groundwater are often much smaller than the ones used in our experiments (Harvey and Garabedian, 1991), and the particle size has a marked influence on particle migration.

5. Conclusions

Transport of bacteria under unsaturated conditions is reduced due to their tendency to attach to air–water interfaces. Because the bacterial affinity to air–water interfaces is larger than their affinity to solid surfaces, this process may largely control bacterial mobility in unsaturated soils. Mechanistic model development is useful to identify factors that influence bacterial transport in porous media. The changes in available area of both solid and air–water interfaces due to bacterial coverage and changes in the water flow have to be considered. Although colloid transport in an unsaturated matrix is still not sufficiently understood to account for all processes, an exact description of the hydraulic properties helps to characterize the flow properties of the system.

References

Adamson, A.W., 1990. Physical Chemistry of Surfaces. Wiley, New York.

Blanchard, D.C., Syzdek, L.D., 1972. Concentration of bacteria in jet drops from bursting bubbles. J. Geophys. Res. 77, 5087–5099.

Champ, D.R., 1986. Microbial mediation of radionuclide transport. In: Molz, F.H., Mercer, J.W., Wilson, J.T. (Eds.), Abstracts of the AGU Chapman Conference on Microbial Processes in the Transport, Fate, and In-Situ Treatment of Subsurface Contaminants, Snowbird, Utah. American Geophysical Union, Washington, DC, p. 17.

Corapcioglu, M.Y., Choi, H., 1996. Modeling colloid transport in unsaturated porous media and validation with laboratory column data. Water Resour. Res. 32, 3437–3449.

Dahlbäck, B., Hermansson, M., Kjelleberg, S., Norkrans, B., 1981. The hydrophobicity of bacteria—an important factor in their initial adhesion at the air–water interface. Arch. Microbiol. 128, 267–270.

Derjaguin, B.V., Landau, L., 1941. Theory of the stability of strongly charged lyophobic sols and the adhesion of strongly charged particles in solutions of electrolytes. Acta Physicochem. URSS 14, 633.

Ducker, W.A., Xu, Z., Xu, N., Xu, I.J., 1994. Measurements of hydrophobic and DLVO forces in bubble-surface interactions in aqueous solutions. Langmuir 10, 3279–3289.

Dury, O., Fischer, U., Schulin, R., 1998. Dependence of hydraulic and pneumatic characteristics of soils on a dissolved organic compound. J. Contam. Hydrol. 33, 39–57.

Gerba, C.P., Yates, M.V., Yates, S.R., 1991. Quantification of factors controlling viral and bacterial transport in the subsurface. In: Hurst, C.J. (Ed.), Modeling the Environmental Fate of Microorganisms. American Society of Microbiology, Washington, DC, pp. 77–88.

Gvirtzman, H., Roberts, P.V., 1991. Pore scale spatial analysis of two immiscible fluids in porous media. Water Resour. Res. 27, 1165–1176.

Harvey, R.W., Garabedian, S.P., 1991. Use of colloid filtration theory in modeling movement of bacteria through a contaminated aquifer. Environ. Sci. Technol. 25, 178–185.

Hiemenz, P.C., 1986. Principles of Colloid and Surface Chemistry. Marcel Dekker, New York.

Huysman, F., Verstraete, W., 1993. Water-facilitated transport of bacteria in unsaturated soil columns: influence of inoculation and irrigation methods. Soil Biol. Biochem. 25, 91–97.

Jewett, D.G., Logan, B.E., Arnold, R.G., Balea, R.C., 1996. Bacterial transport through unsaturated quartz sand and the effects of ionic strength and surfactant addition. AGU Meeting, EOS, San Francisco, p. F210.

Johnson, P.R., Elimelech, M., 1995. Dynamics of colloid deposition in porous media: blocking based on random sequential adsorption. Langmuir 11, 801–812.

Klute, A., Dirksen, C., 1986. Hydraulic conductivity and diffusivity: laboratory methods. In: Klute, A. (Ed.), Methods of Soil Analysis. Soil Science Society of America, Madison, WI.

Lindqvist, R., Bengtsson, G., 1991. Dispersal dynamics of groundwater bacteria. Microb. Ecol. 21, 49–72.

Liu, D., Johnson, P.R., Elimelech, M., 1995. Colloid deposition dynamics in flow through porous media: role of electrolyte concentration. Environ. Sci. Technol. 29, 2963–2973.

Marshall, K.C., Cruickshank, R.H., 1973. Cell surface hydrophobicity and the orientation of certain bacteria at interfaces. Arch. Mikrobiol. 91, 29–40.

Martin, R.E., Bouwer, E.J., Hanna, L.M., 1992. Application of the clean-bed filtration theory to bacterial deposition in porous media. Environ. Sci. Technol. 26, 1053–1058.

McCarthy, J.F., Zachara, J.M., 1989. Subsurface transport of contaminants. Environ. Sci. Technol. 23, 496–502.

Powelson, D.K., Mills, A.L., 1996. Bacterial enrichment at the air–water interface of a laboratory apparatus. Appl. Environ. Microbiol. 62, 2593–2597.

Reeves, P.C., Celia, M.A., 1996. A functional relationship between capillary pressure, saturation, and interfacial area as revealed by a pore-scale network model. Water Resour. Res. 32, 2345–2358.

Reichert, P., 1994. AQUASIM—a tool for simulation and data analysis of aquatic systems. Water Sci. Technol. 30, 21–30.

Rijnaarts, H.H.M., Norde, W., Bouwer, E.J., Lyklema, J., Zehnder, A.J.B., 1995a. Reversibility and mechanism of bacterial adhesion. Colloid Surf. B 4, 5–22.

Rijnaarts, H.H.M., Norde, W., Lyklema, J., Zehnder, A.J.B., 1995b. The isoelectric point of bacteria as an indicator for the presence of cell surface polymers that inhibit adhesion. Colloid Surf. B 4, 191–197.

Rijnaarts, H.H.M., Norde, W., Bouwer, E.J., Lyklema, J., Zehnder, A.J.B., 1996. Bacterial deposition in porous media related to the clean bed collision efficiency and to substratum-blocking by attached cells. Environ. Sci. Technol. 30, 2869–2876.

Rittmann, B.E., 1994. In Situ Bioremediation, 2nd edn. Noyes Publishers, Park Ridge, NJ.

Saripalli, K.P., Kim, H., Rao, P.S.C., Annable, M.D., 1997. Measurement of specific fluid–fluid interfacial areas of immiscible fluids in porous media. Environ. Sci. Technol. 31, 932–936.

Schäfer, A., Harms, H., Zehnder, A.J.B., 1998. Bacterial accumulation at the air–water interface. Environ. Sci. Technol., submitted.

Schraa, G., Bethe, B.M., van Neerven, A.R.W., van den Tweel, W.J., van der Wende, E., Zehnder, A.J.B., 1987. Degradation of 1,2-dimethylbenzene by *Corynebacterium* strain C125. Antonie van Leeuwenhoek 53, 159–170.

Stauffer, F., Dracos, Th., 1986. Experimental and numerical study of water and solute infiltration in layered porous media. J. Hydrol. 84, 9–34.

Tsao, Y.H., Evans, D.F., Wennerström, H., 1993. Long-range attraction between a hydrophobic surface and a polar surface is stronger than that between two hydrophobic surfaces. Langmuir 9, 779–785.

Ustohal, P., Stauffer, F., Dracos, Th., 1998. Measurement and modelling of hydraulic characteristics of unsaturated porous media with mixed wettability. J. Contam. Hydrol. 33, 5–37.

van Genuchten, M.T., Wierenga, P.J., 1976. Mass transfer studies in sorbing porous media: I. Analytical solutions. Soil Sci. Soc. Am. J. 40, 473–480.

van Loosdrecht, M.C.M., Lyklema, J., Norde, W., Schraa, G., Zehnder, A.J.B., 1987a. Electrophoretic mobility and hydrophobicity as a measure to predict the initial steps of bacterial adhesion. Appl. Environ. Microbiol. 53, 1898–1901.

van Loosdrecht, M.C.M., Lyklema, J., Norde, W., Schraa, G., Zehnder, A.J.B., 1987b. The role of bacterial cell wall hydrophobicity in adhesion. Appl. Environ. Microbiol. 53, 1893–1897.

Verwey, E.J.W., Overbeek, J.T.G., 1948. Theory of the Stability of Lyophobic Colloids. Elsevier, Amsterdam.

Wan, J., Tokunaga, T.K., 1996. Film-straining of colloids in unsaturated porous media: conceptual model and experimental testing. AGU Meeting, EOS, San Francisco, p. F211.

Wan, J., Wilson, J.L., 1994. Colloid transport in unsaturated porous media. Water Resour. Res. 30, 857–864.

Wan, J., Wilson, J.W., Kieft, T.L., 1994. Influence of the gas–water interface on transport of microorganisms through unsaturated porous media. Appl. Environ. Microbiol. 60, 509–516.

Williams, D.F., Berg, J.C., 1991. The aggregation of colloidal particles at the air–water interface. J. Coll. Interface Sci. 152, 218–229.

Williams, P.A., Worsey, M.J., 1976. Ubiquity of plasmids in coding for toluene and xylene metabolism in soil bacteria: evidence for the existence of a new TOL plasmid. J. Bacteriol. 125, 818–828.

Wilson, G.Y., Kinsall, B.L., Palumbo, A.V., Burlage, R., Yunsheng, L., 1996. Heterogeneity in physical and hydraulic properties control the unsaturated microbial transport through a vadose zone. AGU Meeting, EOS, San Francisco, p. F211.